

# Surface plasmon polaritons interference excited by a tightly focused and radially polarized vortex beam

MA WEN-JUAN, ZOU WEN-DONG\*, HUANG PIN-BO, WANG WEI-HONG

*Key Laboratory of Nondestructive Test (Ministry of Education), Nanchang Hangkong University, Nanchang, 330063, Jiangxi, China*

A tightly focused and radially polarized vortex beam can not only provide a wider angular spectrum and a stronger longitudinal electric field in the process of surface plasmon polaritons (SPPs) interference, but also avoid the influence of the center angular spectrum on the main peak of the SPPs interference field. In this paper, we focus on a case of a SPPs standing field induced by a tightly focused and normally incident radially polarized vortex beam and compare it with that resulting from radially polarized Gaussian beam and linear polarized vortex beam. At the present time, the photonic nano-devices based on the SPPs are considered to be the basic of all-optical integrated loop with nanometer scale. So the study of the properties of the SPPs standing field is very important and some factors on the generation of interference pattern is considered and analyzed.

(Received November 1, 2012; accepted June 12, 2013)

*Keywords:* Tightly focusing, Surface plasmon polaritons (SPPs), Vortex beam, Radially polarized

## 1. Introduction

Under certain condition the photons of incident light interact with the free electrons of the metal film to generate collective resonance each other and excite surface electromagnetic wave propagating along the dielectric/metal interface, which is the surface plasmon polaritons (SPPs) [1]. The local SPPs is a kind of excited evanescent wave which is decaying exponentially perpendicular to the interface due to boundary conditions. The effect has a wide range of applications in many fields such as nanoscale optical devices, ultrahigh sensitivity biosensing, new sub-wavelength lithography system and so on [2-5] for its innate characteristic. When utilizing Gaussian beam [6,7] that normally focuses on a metal film to generate surface plasmon polaritons (SPPs), the transmitted field component of Gaussian beam can confuse the SPPs standing wave field. However, the vortex beam which has a dark spot in the center can avoid the influence and attracts much researcher's attention [9,10]. The P. S. Tan's group obtained the SPPs interference pattern by linear polarized vortex beam [11]. According to the characteristics of the high numerical aperture system, the tightly focused beam can provide a larger incidence angle spectrum. Therefore, we recommended study the properties of SPPs interference field induced by a tightly focused and radially polarized vortex beam with normal incidence. In addition, to improve the parameter indexes, it is necessary to analyze some effects of some important factors on the doughnut

SPPs standing wave field.

## 2. Theory

The pivotal problem for exciting SPPs is the dispersion relation. The wavevector of SPPs is greater than the one of light with the same frequency and therefore it can not be directly excited by light. In fact, there are two ways to generate evanescent wave with exciting light of greater wave vector. One is grating coupler, in which a portion of the incident light diffracting the metal slit may gain additional energy along the film surface to excite SPPs. The other one is to use attenuated total reflection (ATR) to form transmitted evanescent wave on the basis of the Otto or Kretschman model. Nevertheless, the SPPs standing wave is restricted by many factors, one of which is the incident beam. Utilizing vortex beam can avoid the participation of the center angular spectrum, protrude the interfering signal of SPPs and get a distinct SPPs interference annulus.

The reason is that the vortex beam has special characters of continuous helical phase singularities and its field intensity in the dark spot is to be zero. The vortex beam can generate by passing through an azimuthally modulated phase mask or mode conversions [11] and we can get a phase of  $\exp(il\varphi)$  where  $l$  is the topological charge [12]. Therefore, we consider a tightly focused and self-interference radially polarized vortex beam vertically illuminate on an metal/air interface for

the reason that the radial polarization is different from linear polarization and azimuthal polarization which is p-polarized component can exist in the every direction. Furthermore, the radially polarized and tightly focused beam not only can produce smaller focal point than the other different polarization states, but it is also with a stronger longitudinal electric field in the region of focal point. And the mathematical expression of radial polarization along radial is given by

$$\mathbf{E}_{inc} = E_0 \exp(il\phi) [\cos\phi \cdot \mathbf{x} + \sin\phi \mathbf{y}] \quad (1)$$

Where  $\mathbf{E}_{inc}$  is the incident field supposed to be entirely polarized along the radial, its phase is  $\exp(il\phi)$ . As shown in Fig. 1, it's a schematic diagram of SPPs wave generated by a radially polarized vortex beam. It is guided through the focusing lens and converging toward the origin of the Au/air interface located at the geometric focal plane.

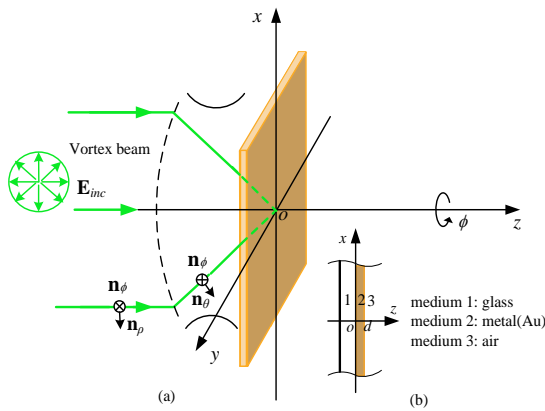


Fig. 1. The schematic diagram of SPPs generated by a radially polarized and tightly focused vortex beam on an Au/air interface(a); the structure of glass/metal(Au)/air (b).

In the high NA modeling system, according to vectorial Debye integral of Richards and Wolf [13,14], the diffracted field near the focal plane can be calculated and expressed as

$$\mathbf{E}_t(x, y, z) = A \iint_{k_x, k_y} t^p(k_{zj}) (\mathbf{E}_{inc} \cdot \mathbf{n}_\rho) \mathbf{n}_\theta \frac{\sqrt{k_{z1}/k_1}}{k_{z1}} \exp[i(k_x x + k_y y + k_{z3} z)] dk_x dk_y \quad (2)$$

where  $A$  is a constant,  $k_x$ ,  $k_y$ ,  $k_{zj}$  are the reciprocal coordinates and  $j=1, 2, 3$  represents the individual medium in different domain, i.e. 1 = glass, 2 = Au and 3 = air.  $\mathbf{n}_\rho$  is the unit vector of a cylindrical coordinate system, whereas  $\mathbf{n}_\theta$  represent the unit vector of a spherical coordinate system, as shown in Fig. 1. Subsequently, inserting Eq. (1) into Eq. (2) and according to the angular

spectrum representation of the vertical component of transmitted field in spherical coordinates  $(\theta, \phi, z)$  is given by

$$E_t(\rho, \phi) \propto \int_0^{\theta_{max}} \int_0^{2\pi} t^p E_0 \sin^2 \theta (\cos \theta)^{1/2} \exp[i(l\phi + k_{z3}d + k_\rho \rho \cos(\phi - \varphi))] d\theta d\phi \quad (3)$$

The tangential vector  $k_\rho = k_1 \sin \theta$ ,  $\theta$  is the divergence angle of the conjugate ray and the maximum divergence angle is  $\theta_{max} = \sin^{-1}(NA/n_1)$ . To consider this effect, the amplitude transmission coefficient of the three-layered system is given by

$$t^p = \frac{4 \exp[i(k_{z2} - k_{z3})d]}{(1 + p_{12})(1 + p_{23})[1 + r_{12}r_{23} \exp(i2k_{z2}d)]}$$

$$p_{ij} = \frac{\varepsilon_i k_{zj}}{\varepsilon_j k_{zi}}, r_{ij} = \frac{1 - p_{ij}}{1 + p_{ij}}, k_{zj} = \sqrt{k_j^2 - k_\rho^2} \quad (4)$$

where  $d$  is the thickness of the gold film.

### 3. Numerical analysis

In this paper, the dielectric constant of glass, gold film and air are  $\varepsilon_1 = 2.31$ ,  $\varepsilon_2 = -5.28 + 2.04i$  (at the incident wavelength of 532 nm),  $\varepsilon_3 = 1$ , respectively. And the gold film thickness is chosen to be 45nm, furthermore, the topological  $l$  is 1 and the numerical aperture is 1.2. Without special statement, these parameters remain the same.

From the Fig. 2(a), the numerical simulation results indicate that when the radially polarized vortex beam vertically focused on the interface of Au/air, the interference pattern of SPPs which is a ring have primary intensity will be generated on the lower surface of Au film without any special structure or holes. Then the SPPs field intensity diminishes quickly with the increasing of the order of annular interference stripe. This phenomenon can be explained by the dispersion relation of SPR that is caused by the existence of gold film ohmic losses. The distribution of SPPs field intensity at x-direction is shown in Fig. 2(b). The radius of zero order SPPs interference fringe is approximate to 250 nm that less than half of incident wavelength. In addition, the electromagnetic field in the inner ring of the vortex beam is nearly equal to zero, which gets rid of

contributions of vertical transmitted lights. However, traditional Gaussian beam can't realize it.

lithography technology, etc.

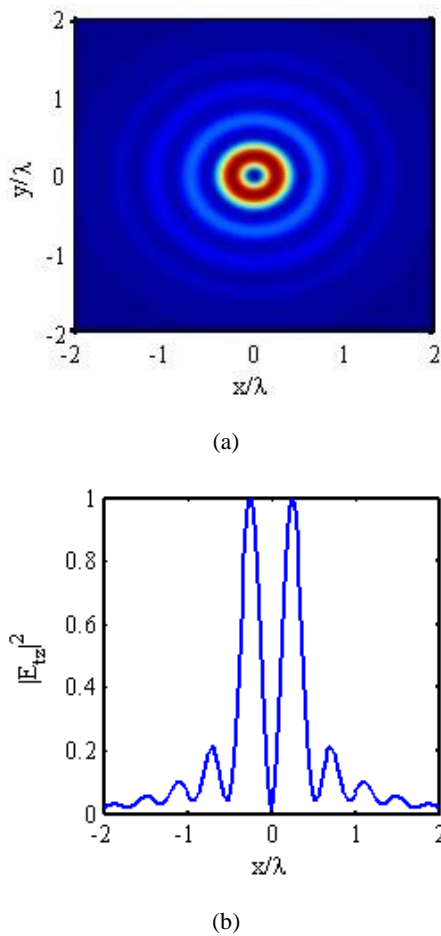


Fig. 2. (a) Numerical simulation results of SPPs generated by a radially polarized and tightly focused vortex beam on an Au/air interface; (b) Normalized transverse profiles of SPPs intensity distribution.

From the results of SPPs generated by radially polarized Gaussian beam in the inset of Fig. 3, we found that the normalized field intensity distribution profiles is a axially symmetric single peak and the maximum field intensity  $|E_z|_{\max}^2$  of SPPs in the central. Compare it with the radially polarized vortex beam, we note that there are two main peaks with the same height of SPPs interference ring and its centre intensity is zero. Although the result of Gaussian beam is better to image, the hollow SPPs interference ring has a potential application as biological molecule manipulation, high precision sub-wavelength

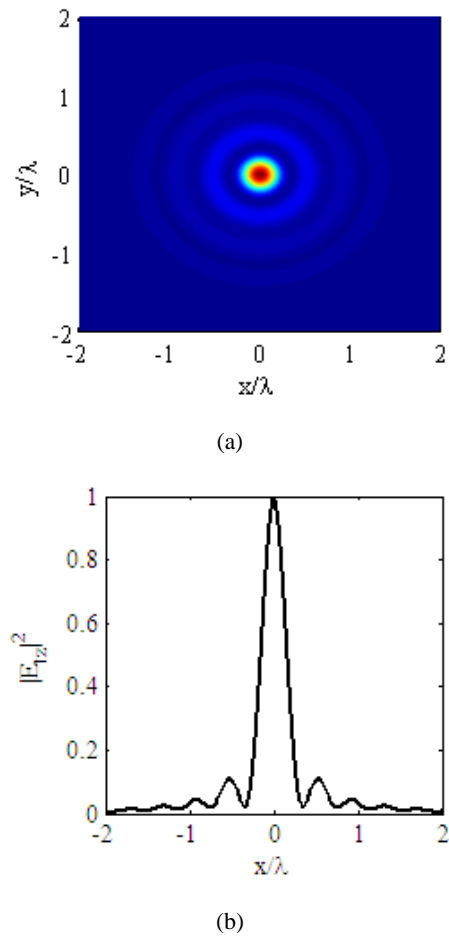


Fig. 3. (a) The results of SPPs induced by a radially polarized Gaussian beam; (b) Normalized SPPs field intensity distribution along x axis.

Besides, the SPPs excited by linearly polarized vortex beam will be considered. As it is shown in the Fig. 4(a), the relative SPPs field intensity distribution profiles is composed of a zero order main peak in the centre and some surrounding high order sidelobes. It is obvious that the maximum SPPs field intensity less than 1. That is, owing to the advantage of the direction, the SPPs field intensity induced by radially polarized vortex beam has higher energy under the same condition.

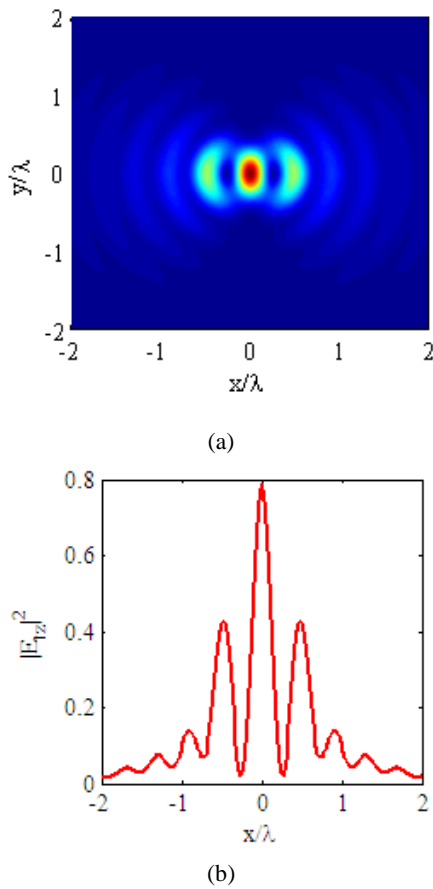


Fig. 4. (a) Calculated the SPPs field for linearly polarized vortex beam; (b) The relative lateral distribution of SPPs field intensity.

Subsequently, the impacts of different factors such as the topological charge  $l$ , the gold film thickness  $d$  and the maximum divergence angle  $\theta_{\max}$  are analyzed and discussed. As it is shown in the Fig. 5, the SPPs field intensity distribution is centrosymmetric. Along with the increase of the topological charge  $l$  the diameter of zero order SPPs interference doughnut about increased from 250nm to 560nm, the SPPs field intensity gradually decreases from 1 to 0.5.

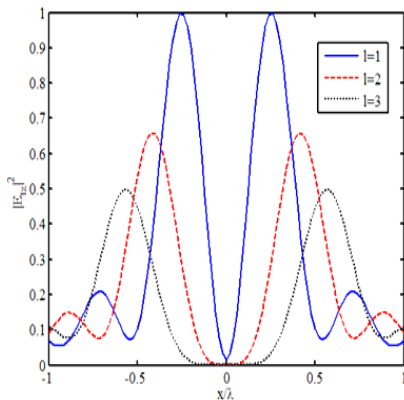


Fig. 5. The lateral distribution curves for the SPPs field intensity for different topological charge.

In addition, along with the increasing thickness  $d$  of gold film, the distance of the two main peaks of annular SPPs field is approximately the same and the main peak increases first and then decreases as shown in Fig. 6. The results indicate that there is an optimized value of gold film thickness  $d$  in this process that is the SPR effect muster with different angular spectrum under the limited of relevant energy spectrum, a compromised solution can be obtained.

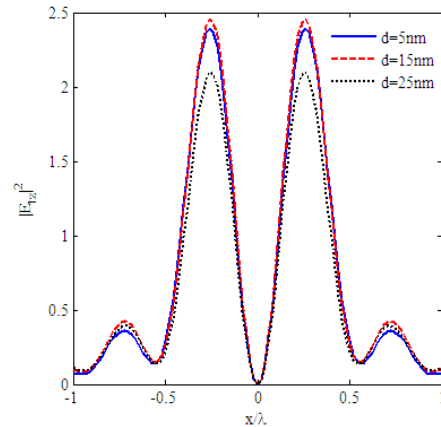


Fig. 6. The lateral distribution curves for the SPPs field intensity with the different gold film thickness.

The numerical simulation results in Fig. 7 revealed that the SPPs standing field strongly depends on the distribution of the angular spectrum energy and with the increasing maximum divergence angle of incidence  $\theta_{\max}$ , the intensity of the SPPs increase rapidly as well. Simultaneously, the two main peak moves to the centre. Thus the SPPs field intensity and magnitude of interference fringe can be modulated by changing the maximum divergence angle  $\theta_{\max}$ . Furthermore, the consequence confirmed that the energy of SPPs standing field also influence by the focus of incident beam except the impact of SPPs effect.

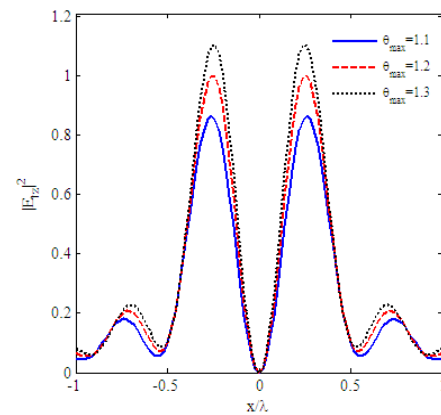


Fig. 7. The lateral distribution of the SPPs field intensity with the maximum divergence angle  $\theta_{\max}$ .

#### 4. Conclusion

Tightly focused and radially polarized vortex beam.

In this paper, we deduce the expression of the diffraction field near the focal plane in the Cartesian coordinate and spherical coordinates respectively. Using the tightly focused and radially polarized vortex beam instead of Gaussian beam to avoid the influence of the transmitted field component on SPPs field and a symmetrical SPPs interference ring have obtained. In addition, we compared it with the radially polarized Gaussian beam and linearly polarized vortex beam, the radially polarized vortex beam is regnant. It also has an important significance in near-field optic imaging system, subwavelength optical sorting, sub-wavelength photolithography, biological molecule manipulation and so on. Especially, different factors of the doughnut SPPs standing wave field are analyzed and some important conclusions and features have been obtained.

#### Acknowledgement

This work is supported by National Natural Science Foundation of China under grant No. 51241005, Natural Science Foundation of Jiangxi Province, China (Grant No. 2008GZW0011, No.20122BAB202010), The Industry Project of Science & Technology Pillar Program of Jiangxi Province, China (Grant No.20122BBE500040).

#### References

- [1] H. Raether, Springer Tracts in Modern Physics, (Springer, Berlin, 1988).
- [2] L. Uo X, Ishihara T, Appl. Phys. Lett., **84**, 4782 (2004).
- [3] E. Chung, D. K. Kim, P. T. C. So, Opt. Lett. **31**, 945 (2006).
- [4] Humeyra Caglayan, Irfan Bulu, and Ekmel Ozbay, J. Appl. Phys. **103**, 053105 (2008).
- [5] K. J. Moh, X.-C. Yuan, J. Bu, S. W. Zhu, B. Z. Gao, Opt. Lett. **34**(7), 971 (2009).
- [6] A. Bouhelier, Opt. Lett. **32**, 2535 (2007).
- [7] Häfele, V. Applied Physics Letters. **101**, 20, 201102-201102-4 (2012).
- [8] Hiroshi Kano, Topics Appl. Phys. **81**, 189 (2001).
- [9] Q. W. Zhan, Opt. Lett. **31**, 1726 (2006).
- [10] P. S. Tan, X.-C. Yuan, G. H. Yuan, Q. Wang, Appl. Phys. Lett. **97**, 241109 (2010).
- [11] P. S. Tan X.-C. Yuan, J. Lin, et al., Opt. Express. **16**, 18451 (2008).
- [12] R. J. Beck, J. P. Parry, W. N. MacPherson, et al, Optics Express., **18**(16), 17059 (2010).
- [13] B. Richards, E. Wolf, Proc. Roy. Soc. (London). A **253**, 358 (1959).
- [14] E. Wolf, Proc. Roy. Soc. Ser. (London). A **253**, 349 (1959).

---

\*Corresponding author: 18979106189@189.cn